Annals of Glaciology 17 1993
© International Glaciological Society

Characterization of a hoar-development episode using SSM/I brightness temperatures in the vicinity of the GISP2 site, Greenland

CHRISTOPHER A. SHUMAN, RICHARD B. ALLEY AND SRIDHAR ANANDAKRISHNAN
Earth System Science Center and Department of Geosciences, The Pennsylvania State University, University Park, PA 16802, U.S.A.

ABSTRACT. Formation of a surface-hoar/depth-hoar complex at the GISP2 site in central Greenland was correlated with large changes in Special Sensor Microwave/Imager (SSM/I) brightness–temperature data. Pass-averaged SSM/I brightness-temperature data over a 1/2° latitude by 1° longitude cell for the 19 and 37 GHz, vertically (V) and horizontally (H) polarized bands were manipulated to yield differential (V–H) trends which clearly show a gradual decline as the hoar formation caused a progressively rougher surface with progressively lower density. The hoar episode ended as snowfall, and high winds buried and destroyed the surface-hoar layer and caused rapid V–H increases in ≈ 1 day. Comparison of the different trends with changes in the field-monitored variables and theoretical values suggest that the V–H trends are sensitive primarily to changes in surface roughness, and secondarily to near-surface density changes. Consistent expression of trends in microwave brightness temperature over 35 adjacent study cells indicates that this technique may provide a remote-sensing signature capable of defining the timing and spatial extent of surface- and depth-hoar formation in central Greenland.

INTRODUCTION

Passive-microwave remote sensing is an effective means of evaluating the spatial characteristics of snow and ice in glaciological studies (Rees and Squire, 1989), especially in polar regions (Fily and Benoist, 1991). However, because microwave remote-sensing techniques sample polar firn to some depth, accurate analysis of the remote-sensing signal is critically dependent on knowledge of firn characteristics through time (Alley, 1987; Colbeck, 1991). This sampling depth may include hoar complexes used to define annual layering (Benson, 1962; Taylor and others, in press) and other stratigraphic markers observed in snow pits and ice cores. Previous research has demonstrated that density and roughness variations related to hoar formation and wind action at and near the surface of the firn can influence passive-microwave signals (Hall, 1987; Remy and Minster, 1991). The investigation presented here was prompted by the observation of hoar formation at the surface and at depth during June and July 1990 at the GISP2 site in central Greenland (Alley and others, 1990). In this paper we show the relationship of microwave-signal variations to changes at and near the firn surface, and speculate on their cause.

SSM/I DATA

To analyze the effects of hoar development on passive-microwave signals, SSM/I data from the 19 GHz (1.55 cm) and 37 GHz (0.81 cm), vertically (V) and horizontally (H) polarized bands were obtained for an approximately 70 000 km^2 region. Unfortunately no reliable 85 GHz data were available for this time period. The study region, between 71° and 74° N and 36° and 42° W, was subdivided into 36 cells (Fig. 1). A two-part processing routine was used to subset geographically and to pass-average the raw brightness-temperature data provided by Remote Sensing Systems of Santa Rosa, California. During the 61-day period selected for study (midnight 31 May to midnight 31 July 1990), 775–900 SSM/I observations per cell were pass-averaged to produce 220–300 mean values. These means represent from one to six observations from each SSM/I orbital pass over a cell in the coverage region.

Plots of the resulting brightness-temperature trends for Cell 16, which covers the GISP2 site, reveal that all four bands record a general warming of 5–10 K through increased microwave emission during the study period (Fig. 2). This overall warming trend is supported by daily average temperature data from automatic weather station Kenton (south of GISP2 in Cell 22) and (V + H)/2 brightness-temperature trends for the 19 and 37 bands (Fig. 3). On 20 June the 37 V band began a 4–5 K decline in brightness temperature. The 19 V band mirrored changes in the 37 V band data but with reduced magnitude (2–3 K decrease). Both declines gradually reversed about 6–8 July. In contrast, the H-band brightness temperatures began to increase on 20 June, rising 8–9 K for the 37 H band and 6–7 K for the 19 H band. A rapid, approximately one-day, drop of ≈9 K and

https://doi.org/10.3189/S0260305500012817 Published online by Cambridge University Press

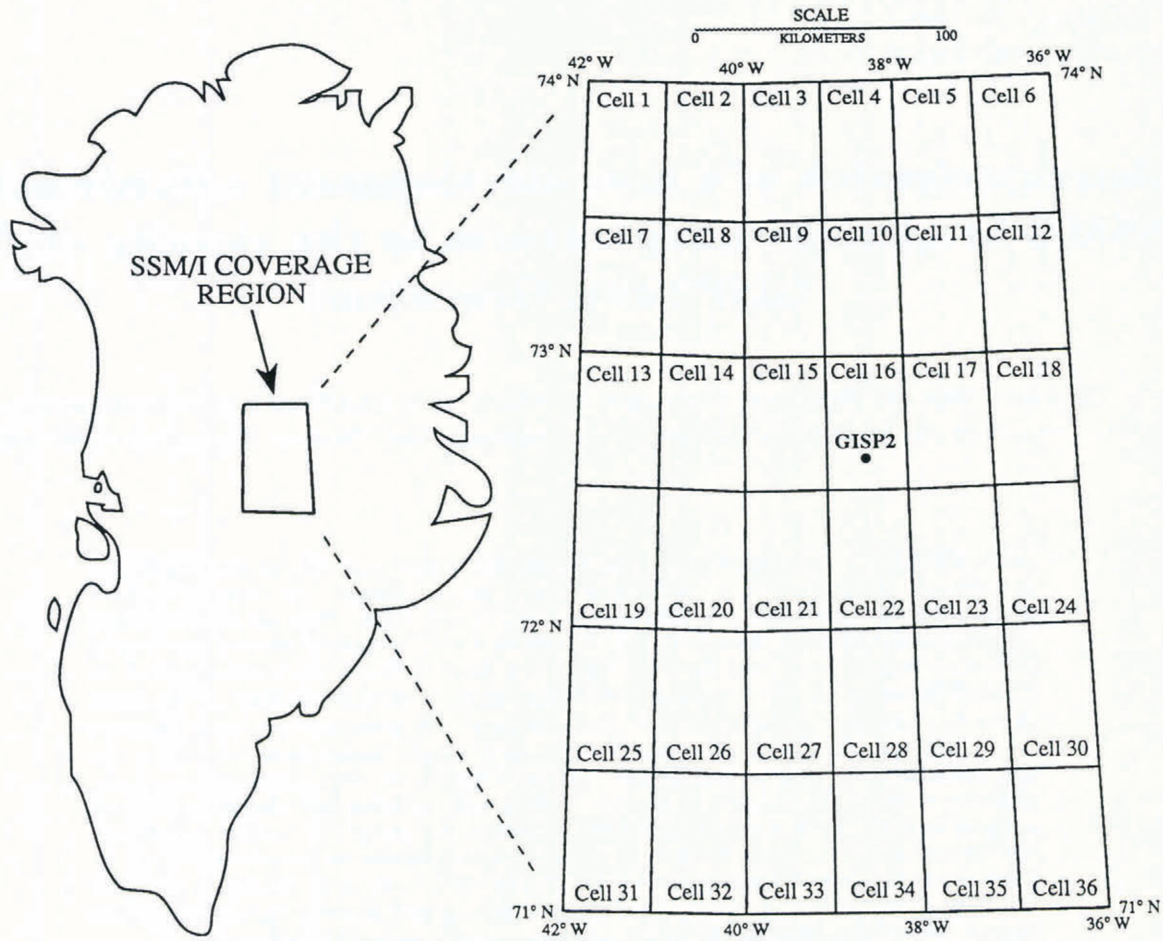

Fig. 1. Location of SSM/I coverage region and study cells in relation to central Greenland and the GISP2 site.

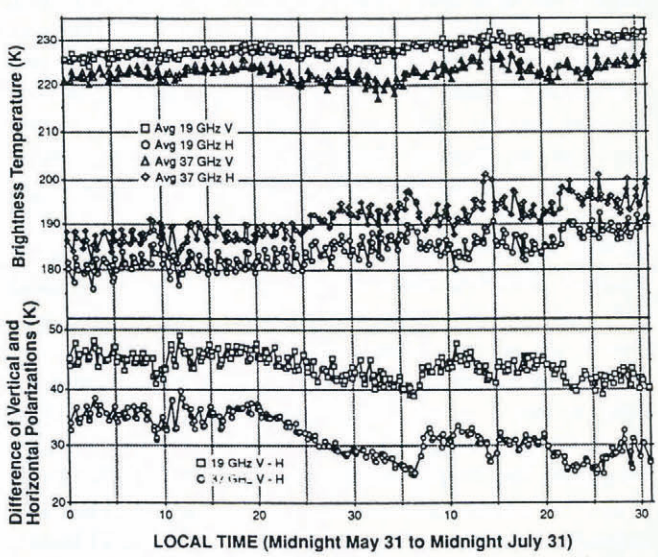

Fig. 2. Trends of pass-averaged SSM/I brightness temperatures for the 19 and 37 GHz, vertically (V) and horizontally (H) polarized bands, and the resulting differential (V–H) data over the 61 day study period for Cell 16.

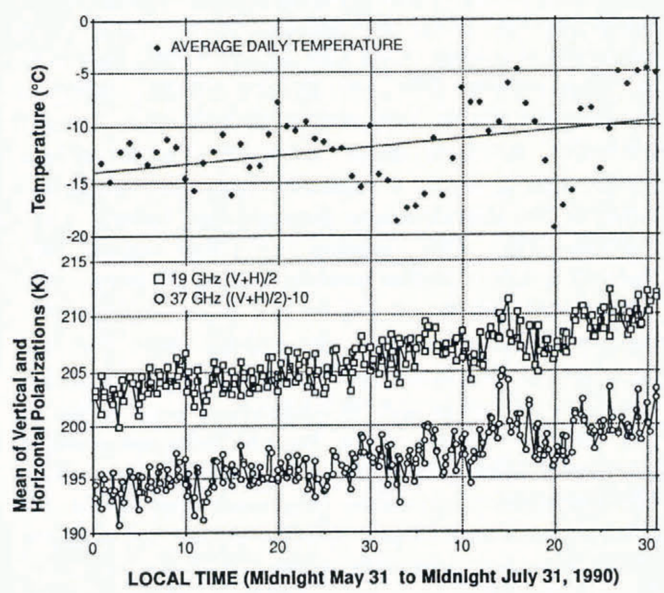

Fig. 3. Trends of near-surface air temperature at automatic weather station Kenton and $(V + H)/2$ brightness temperatures for the 19 and 37 GHz bands over the 61 day study period for Cell 16. Note: the 37 data have been offset by 10 K for presentation clarity, and the regression line defines the air temperature trend during the study period. Air-temperature data are courtesy of C. Stearns.

https://doi.org/10.3189/S0260305500012817 Published online by Cambridge University Press

≈6 K for the 37 H and 19 H bands, respectively, occurred on 7–8 July. Examination of similar plots for the data from the other 35 study cells indicates that these changes are generally consistent across the entire study area.

To show critical changes in the brightness-temperature trends, the 19 and 37 band pass-averaged data were manipulated to produce separate differential (V–H) plots for each cell. These plots reveal a gradual drop between 20 June and 7 July of ≈12 K and ≈8 K for the 37 and 19 GHz band differentials, respectively. The gradual decline of the differential values abruptly terminated about 8 July with a rapid one-day increase of ≈8 K for the 37 GHz band data and a corresponding ≈5 K increase in the 19 GHz band data.

FIELD DATA

Changes in near-surface snow conditions were monitored near the GISP2 site from 18 June to 14 July 1990. Numerous (typically 10–20 per day) shallow (typically 10–20 cm) snow pits were excavated and examined most days, and general appearances were recorded. Samples for volume-mass determination of density were collected using box samplers of 1 cm or 3 cm thickness. Owing to the fragility and irregular thickness of surface hoar, most samples included hoar and overlying air, giving a lower limit on the true density, or surface hoar and underlying material that appeared denser on inspection, giving an upper limit on the true density. Some thin sections were prepared and examined, although their value was limited because the surface hoar was altered mechanically during impregnation with liquid dimethyl phthalate. Samples were collected for chemical and isotopic analyses, and a few detailed temperature profiles were measured from about 1 m above the snow surface to 1 m depth. Some of these observations were extended into pits 2 m deep. Some data are presented in Alley and others (1990) and Figure 4; other data are still under analysis.

Surface roughness related to hoar development (Fig. 5) was monitored by inspection, although no quantitative measurements were made during the study period. At all times the surface contained low-amplitude dunes or sastrugi (<10 cm) of long wavelength (>1–10 m) and submillimetric grain-scale roughness. Subsequent surface-hoar growth caused a prominent, popcorn-like roughness with wavelength and amplitude on the order of 1 cm. The observed changes in this scale of roughness are illustrated in Figure 4.

Following a series of wind- and snowstorms at GISP2 that ended late on 19 June, a period of warm, still weather led to the formation of a near-surface complex of surface and depth hoar (Fig. 4). Starting on 20 June near-surface density in the hoar complex declined whereas depth-hoar and surface-hoar thickness increased and the surface became increasingly rough at the centimetric scale. A thin layer of new snow was deposited on 28–29 June which filled in between the existing surface-hoar crystals and caused an abrupt decrease in centimeter-scale surface roughness. Little apparent change in near-surface density was noted at this time, however. Surface-hoar growth resumed almost immediately and the new snow was progressively metamorphosed until it was not separately identifiable.

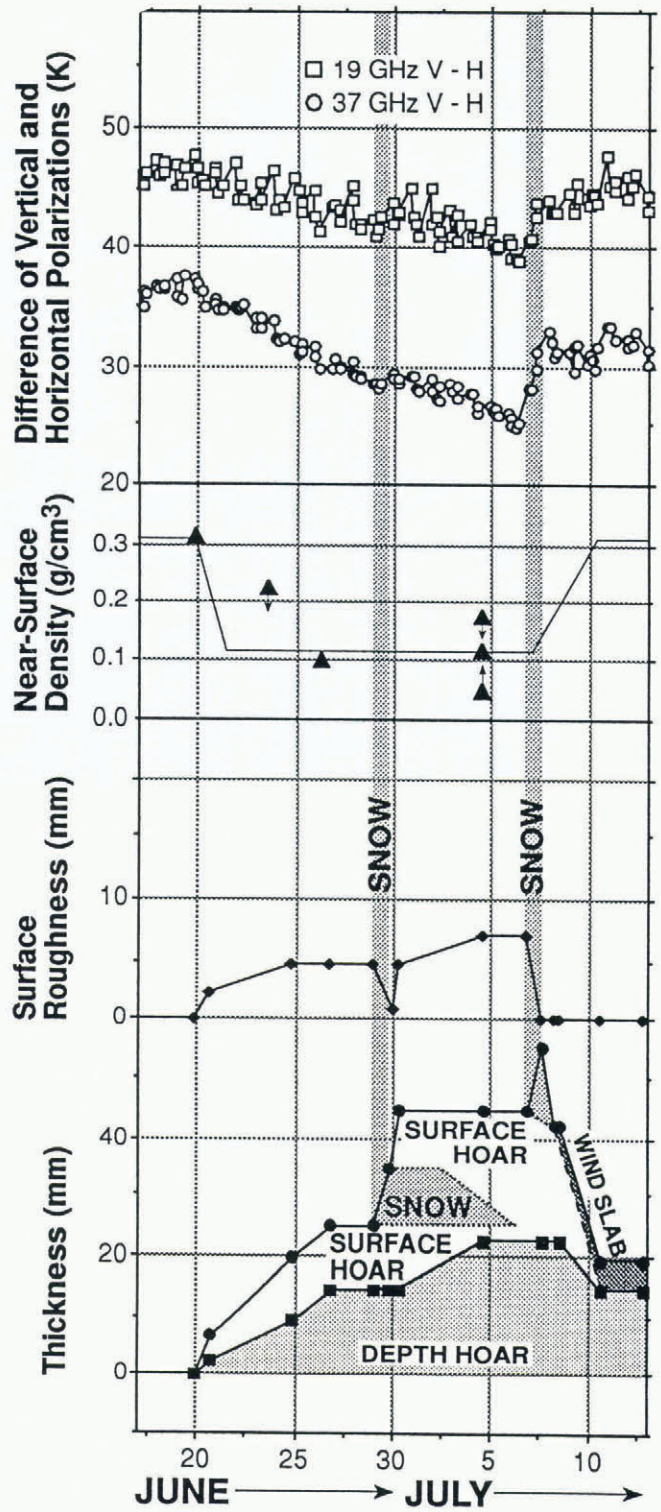

Fig. 4. Plot showing the temporal relationship of the V–H differential trends to near-surface density, centimeter-scale surface roughness, surface- and depth-hoar layer thicknesses, and snow and wind events (trends are constrained by additional observations later in July). Density points with attached arrows are limiting values; the true values plot in the direction of the arrow.

The hoar complex continued to thicken and surface roughness increased through the first week in July until a second snowfall on 6–8 July, an event which also filled in the surface hoar and again decreased surface roughness,

https://doi.org/10.3189/S0260305500012817 Published online by Cambridge University Press

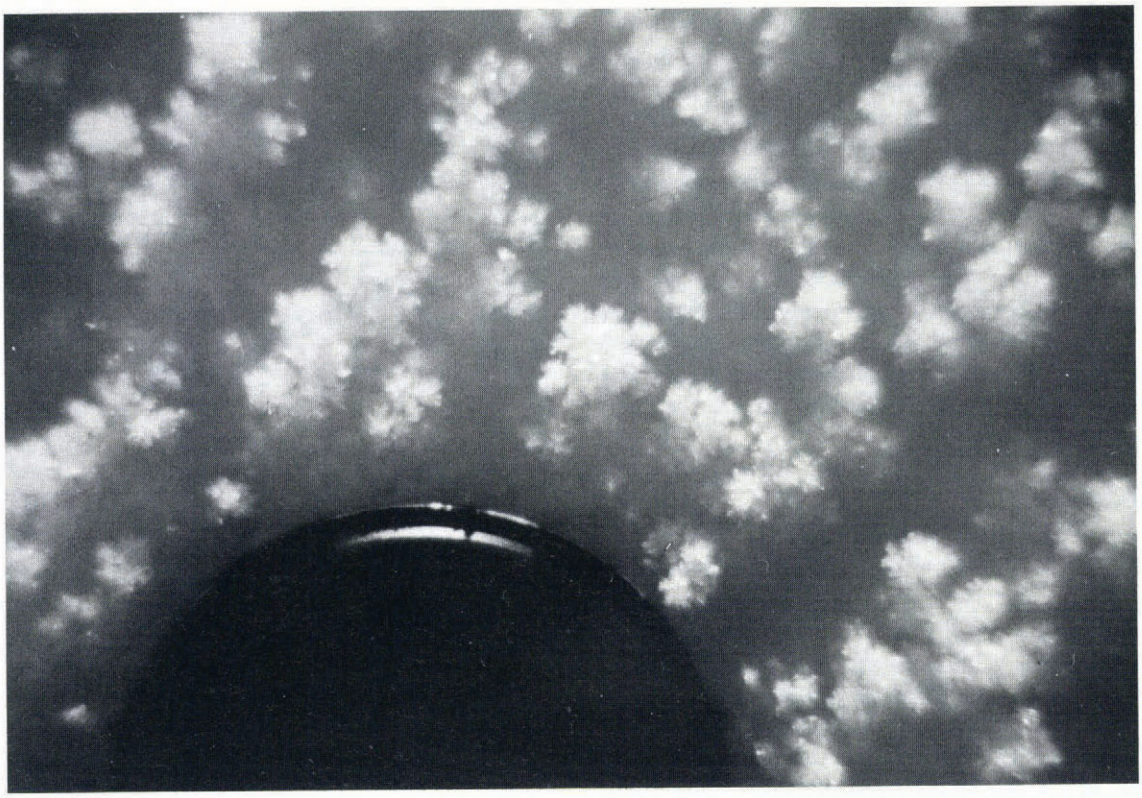

Fig. 5. Photograph of developing surface-hoar crystals near the GISP2 camp on 24 June 1990 at about 2100 h. The lens cap is approximately 65 mm in diameter.

with little apparent effect on surface density. This was followed by an increasingly windy period that caused an increase in the surface density but had little effect on surface roughness. The new snow was reworked into a variably thick wind crust/wind slab by 8 July, which was progressively thinned and reworked until the accumulated surface hoar and even some of the depth hoar were removed by 15 July. This left the surface as a dense, relatively smooth wind slab thinning locally to a mm-thick wind crust (Fig. 4).

ANALYSIS

Remy and Minster (1991) used Scanning Multichannel Microwave Radiometer (SMMR) passive-microwave data from Antarctica to develop a model explaining V–H differentials. They argued that observed brightness temperatures over ice sheets are less than expected for a black-body radiating at the in-situ temperature because of volume scattering (including any reflections from internal interfaces) within the upper meter(s) sampled by the radiometer, and because of reflection of radiation from below at the snow–air interface. Any energy that is scattered or reflected downward is not emitted, so reflection and scattering decrease the observed brightness temperature.

Reflection is primarily a function of surface density, surface roughness, incidence angle, and polarization. At the SSM/I sensor's incidence angle of 53.1° (Hollinger and others, 1987), surface reflection from a specular surface is almost zero for the vertical polarization, regardless of other conditions, but may be significant for the horizontal polarization. Thus, more brightness-temperature variability is expected in the H channels than in the V channels (Remy and Minster, 1991), as is observed in this study.

Efficient downward reflection of the H channel causes these brightness temperatures to be low, and the resulting V–H differential to be large. Reflection at the snow–air interface is efficient if the dielectric contrast across the surface is high, which occurs when the snow density is high. Reflection also is efficient when the surface is smooth; a rough surface does not provide a good specular reflector (Remy and Minster, 1991). Thus, a decrease in surface density or an increase in surface roughness should cause a decrease in V–H by increasing emitted horizontally polarized microwave radiation.

Remy and Minster note that volume scattering may affect brightness temperature significantly, as proposed by Zwally (1977), but they do not model effects of volume scattering on V–H differentials. Effects of observed anisotropy in the granular structure of firn (e.g. Alley, 1987) and of reflections off layers within the firn might be significant. However, in our case the observed changes in snow parameters were restricted to the upper few cm of the upper layer of snow, a short distance compared to the depth of one to a few m from which microwaves reach the sensor (Chang and others, 1976; Mätzler, 1987). We thus assume that volume scattering did not change over our experiment, and focus on changes in the near-surface density and roughness as controlling the observed short-period changes in V–H differentials.

Theoretical calculations for a planar, reflective surface at an assumed temperature of 263 K, based on equations 6, 8 and 9 in Remy and Minster (1991), indicate that a

https://doi.org/10.3189/S0260305500012817 Published online by Cambridge University Press

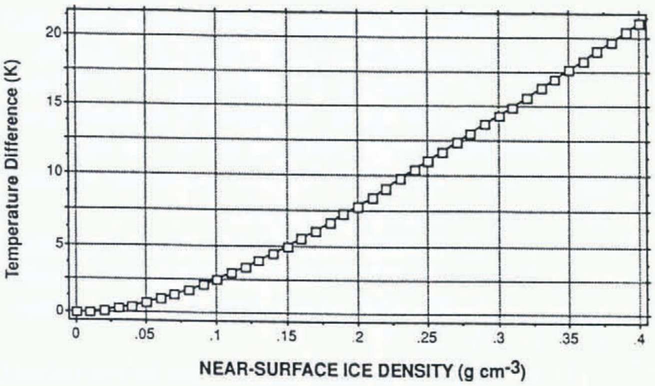

Fig. 6. Theoretical relationship of V–H differential temperature as a function of the near-surface density of a planar reflector at 263°K. Note: as roughness increases, the resulting temperature difference at a given density will decrease. Derived from equations 6, 8 and 9 in Remy and Minster (1992).

surface density of 0.3 g cm^{-3}, such as existed on 19 June, would cause a V–H of about 14 K (Fig. 6). The observed roughness elements on the snow on 19 June were very large (sastrugi) or very small (grain-scale) compared to the wavelengths of the 37 and 19 channels, and thus would have had little effect on the microwave emissions. The observed V–H values through the study period are much larger than 14 K, which suggests that volume scattering (probably including reflections off deeper interfaces) also contributes to the V–H trends; nonetheless, this calculation indicates that short-period changes in V–H should be around 14 K or less, as observed.

Beginning on 20 June, the upper surface of the snow was replaced by two interfaces: (1) a contact between the deeper snow (density approximately 0.3 g cm^{-3}) and the base of the depth hoar (density about 0.15); and (2) a contact between the top of the surface hoar (density about 0.15) and the air. Because the reflection coefficient increases more rapidly than the density difference across an interface (Fig. 6), this should have caused a decrease in reflection of the H polarization and in V–H. The depth hoar initially was spatially discontinuous, and became continuous over several days. Thereafter, it thickened, and material immediately below it coarsened so that its lower contact became increasingly gradational. The effect of this should have been progressive reduction in H reflection from the lower interface, and thus in V–H. At the same time, the upper surface was becoming increasingly rough, which should have progressively reduced the H reflection from that surface, and thus V–H. The net result of these changes is calculated to be a gradual decrease in V–H, as observed. Essentially, the process of hoar formation replaced the discrete surface by a diffuse zone with no clear boundaries, reducing reflection at the surface and thereby reducing V–H.

The small increase in differential temperature beginning on 29 June, and the large increase beginning on 6 July, correlate with periods of snowfall that smoothed the upper interface and would be expected to have increased its reflectivity. A now smooth interface with a density of 0.15 g cm^{-3} could increase V–H by almost 5 K (Fig. 6), enough to account for most of the observed signal. The smoothing on 6 July was followed almost immediately by a density increase of the surface, which may have contributed further to the increase in V–H at this time. It should be noted that V–H does not return to its pre-20 June value. This may be due to two factors: (1) the surface density in July did not rise as high as it did in mid-June; and (2) the high-density surface layer was in some locations a wind crust much thinner than the wavelength and thus nearly transparent to microwaves, effectively leaving a low-density surface in some places for purposes of reflection.

Detailed model calculations to estimate magnitudes of effects are not possible at this time. Because the layer thicknesses are similar to the wavelengths of interest during the hoar-forming period, use of simple theories for specular reflectors is not warranted. Prior to the hoar-forming period, the surface layer was at least several cm and several wavelengths thick, so a simple reflection theory should be approximately valid. Also, we do not have sufficiently detailed data on how sharp the various interfaces were; a gradational interface spanning about 1 cm and one wavelength would reduce reflection significantly compared to a sharp interface with the same roughness and density contrast. The greater sensitivity of the 37 GHz data to near-surface changes compared to the 19 GHz data (Figs 2 and 4) may in part be caused by interfaces appearing graded at the 1.55 cm wavelength of the 19 GHz data but sharp at the 0.81 cm wavelength of the 37 GHz data.

CONCLUSIONS

The difference between brightness temperatures observed in vertically (V) and horizontally (H) polarized channels of the SSM/I radiometer at 37 GHz and 19 GHz varied in close synchrony with changes in near-surface snow conditions at the GISP2 site in central Greenland over about one month of observations during June and July, 1990. Development of a surface-hoar/depth-hoar complex with a very rough upper surface at the cm scale (≈ to the wavelengths studied) caused a strong decrease in the brightness-temperature differential V–H; smoothing of the surface by new snowfall and wind-induced increase in surface density caused an increase in V–H.

Basic physical theory (Remy and Minster, 1991) predicts that a sharp, smooth interface between air and high-density snow should reflect horizontally polarized microwaves emitted by the snow but not affect vertically polarized microwaves at the SSM/I look angle, causing a large V–H. An increase in near-surface roughness and a reduction in near-surface density should decrease reflection of horizontally polarized microwaves with little effect on vertically polarized microwaves, causing a decrease in V–H. The trends observed in V–H parallel those expected from surface observations and this theory, giving considerable confidence that V–H is responding to the changes associated with hoar formation and its burial or removal.

Our knowledge both of the near-surface scattering processes and of the near-surface snow properties is not

https://doi.org/10.3189/S0260305500012817 Published online by Cambridge University Press

sufficient to allow us to predict quantitatively how snow changes will affect the microwave brightness temperatures; further studies are planned. Nonetheless, we believe that with further calibration it will be possible to use V–H data to identify periods of change in surface-snow character on an ice sheet. This should allow improved assessments of firn emissivity and ice-sheet surface temperature in long-term studies of ice-sheet stability and climate sensitivity. In addition, this technique should allow regional characterization of the timing and spatial coherence of the hoar layers which define annual accumulation layers.

ACKNOWLEDGEMENTS

This research was funded in part by grant DPP-8822027 from the U.S. National Science Foundation Division of Polar Programs, as well as by funds from General Electric and the Packard Foundation. We thank the GISP2 SMO and PICO for logistic support, C. Stearns for weather station data, and E. Saltzman for aid in data collection. This is Contribution No. 92-04 of the Greenland Ice Sheet Project (GISP2).

REFERENCES

Alley, R. B. 1987. Texture of polar firn for remote sensing. *Ann. Glaciol.*, **9**, 1–4.

Alley, R. B., E. S. Saltzman, K. M. Cuffey and J. J. Fitzpatrick. 1990. Summertime formation of depth hoar in central Greenland. *Geophys. Res. Lett.*, **17**(12), 2393–2396.

Benson, C. S. 1962. Stratigraphic studies in the snow and firn of the Greenland ice sheet. *SIPRE Res. Rep.* 70.

Chang, T. C., P. Gloerson, T. Schmugge, T. T. Wilheit and H. J. Zwally. 1976. Microwave emission from snow and glacier ice. *J. Glaciol.*, **16**(74), 23–39.

Colbeck, S. C. 1991. The layered character of snow covers. *Rev. Geophys.*, **29**(1), 81–96.

Fily, M. and J.-P. Benoist. 1991. Large-scale statistical study of Scanning Multichannel Microwave Radiometer (SMMR) data over Antarctica. *J. Glaciol.*, **37**(125), 129–139.

Hall, D. K. 1987. Influence of depth hoar on microwave emission from snow in northern Alaska. *Cold Reg. Sci. Technol.*, **13**(3), 225–231.

Hollinger, J., R. Lo, G. Poe, R. Savage and J. Pierce. 1987. *Special sensor microwave imager user's guide.* Washington, DC, Naval Research Laboratory.

Mätzler, C. 1987. Applications of the interaction of microwaves with the natural snow cover. *Remote Sensing Rev.*, **2**(2), 259–387.

Rees, W. G. and V. A. Squire. 1989. Technological limitations to satellite glaciology. *Int. J. Remote Sensing*, **10**(1), 7–22.

Remy, F. and J. F. Minster. 1991. A comparison between active and passive microwave measurements of the Antarctic ice sheet and their association with the surface katabatic winds. *J. Glaciol.*, **37**(125), 3–10.

Taylor, K. *and 6 others.* 1992. Ice-core dating and chemistry by direct-current electrical conductivity. *J. Glaciol.*, **38**(130), 325–332.

Zwally, H. J. 1977. Microwave emissivity and accumulation rate of polar firn. *J. Glaciol.*, **18**(79), 195–215.

The accuracy of references in the text and in this list is the responsibility of the authors, to whom queries should be addressed.

https://doi.org/10.3189/S0260305500012817 Published online by Cambridge University Press